Attempting to Solve the Pigmented Epithelioid Melanocytoma (PEM) Conundrum PRKAR1A Inactivation Can Occur in Different Genetic Backgrounds (Common, Blue, and Spitz Subgroups) With Variation in Their Clinicopathologic Characteristics

Arnaud de La Fouchardiere, Franck Tirode, Christine Castillo, Adrien Buisson, Felix Boivin, Nicolas Macagno, Daniel Pissaloux

Attempting to solve the Pigmented Epithelioid Melanocytoma (PEM) conundrum: PRKAR1A inactivation can occur in different genetic backgrounds (common, blue, and Spitz subgroups) with variation in their clinicopathological characteristics.

Running title: Genetic backgrounds of *PRKAR1A*-inactivated melanocytic tumors.

Arnaud de la Fouchardiere(1,2), Franck Tirode(1,2), Christine Castillo(3), Adrien Buisson(2), Felix Boivin(1), Nicolas Macagno(2,4), Daniel Pissaloux(1,2)

1- Université de Lyon, Université Claude Bernard Lyon 1, INSERM 1052, CNRS 5286, Centre Léon Bérard, Cancer Research Center of Lyon, Equipe Labellisée Ligue contre le Cancer, Lyon, France

2- Department of Biopathology, UNICANCER, Centre Léon Bérard, Cancer Research Center of Lyon, Lyon, France

3- CYPATH, Villeurbanne, France

4 - Aix Marseille Univ, INSERM, APHM MMG, UMR1251, Marmara Institute, Timone University Hospital, Department of Pathology, Marseille, France

Corresponding author:

Arnaud de la Fouchardière, MD, PhD

Department of Biopathology, Center Léon Bérard, 28, rue Laennec, Lyon 69008, France

E-mail: arnaud.delafouchardiere@lyon.unicancer.fr

Acknowledgments:

The authors thank Drs Niel, Mallard, Michiels-Marzais, Durand, Planchard, Ponelle, Pasqualini, Vitte, Youssef Provensal, Poluzzi, Didba, Chevenet, Michalak-Provost, Vilmant, Merchant, Chevallier, Levy, Van Eeckhout, Rey-Buise, Lazzarotto-Rumpler, and Morin for their case contribution, and Drs Darras, Mortier, Vergote, Chevenet, Bouthenet, Touraud and Carena-Damge for their clinical follow-up.

Compliance with ethical standards:

The study was conducted according to the Declaration of Helsinki and has been approved by the research ethics committee of the Center Léon Bérard, Lyon, France (Ref:L21-05).

Conflict of interest:

The authors have disclosed that they have no significant relationships with, or financial interest in, any commercial companies pertaining in this study.

Keywords: Pigmented epithelioid melanocytoma ; PRKAR1A ; BRAF ; GNAQ ; CYSLTR2 ; MAP3K8 ; MAP3K3 ; PEM

Abstract

Pigmented epitheloid melanocytoma (PEM) is a rare cutaneous melanocytic proliferation considered high-grade melanocytoma in the 2018 WHO classification of skin tumors. Little has been reported about the associated genetic drivers in addition to *BRAF* and *MAP2K1* mutations or *PRKCA* gene fusions. Here, we present a series of 21 cases of *PRKAR1A*-inactivated melanocytic tumors in which we could assess the associated genetic background. We identified 9 different driver genes related to the common, Spitz, blue nevi, and *PRKC*-fused groups. Nine cases were associated with a canonical *BRAF* p.V600E mutation, a hallmark of the common nevus group. They occurred mainly in young adults. All were combined (biphenotypic) cases with a variable proportion of compound nevus. The PEM component was made of thin fascicules or isolated epithelioid cells covered by a dense hyperpigmented melanophage background and was predominantly located in the upper dermis. One such case was malignant. Six cases were associated with Spitz-related genetic anomalies ranging from *HRAS* or *MAP2K1* mutations to gene fusions involving *MAP3K8*, *MAP3K3* and *RET*. They occurred mainly in children and young adults. Morphologically, they showed large confluent junctional nests in a hyperplastic epidermis and a fascicular dermal component of spindled and epithelioid melanocytes with a frequent wedged silhouette. Intravascular invasion was observed in 4/6 cases. Five cases were associated with canonical mutations of the blue nevus group with 4 *CYSLTR2* p.L129Q and 1 *GNAQ* p.Q209L mutations. They were removed mainly in adults and showed a frequent junctional component with epidermal hyperplasia. The dermal component showed dense fascicules of spindled and epithelioid melanocytes predominating over melanophages. One case occurred in a *PRKCA*-fused tumor in an adolescent with classic morphological features.

These results could potentially shift the concept of *PRKAR1A*-inactived melanocytoma, changing from a rather unified model to a more complex one, including genetic subgroup variations with clinical and morphological specificities. The genetic background of *PRKAR1A*-inactivated melanocytic tumors should be systematically explored to better understand the extent and clinical behavior of these complex lesions.

Introduction

Pigmented epithelioid melanocytoma (PEM) is a rare melanocytic tumor with specific cytomorphological and genetic criteria. Morphologically, PEMs are defined by a compound melanocytic proliferation with small junctional nests associated with pseudoepitheliomatous hyperplasia of the epidermis. Melanocytes are mid to large in size and epithelioid cytology with a 'fried egg' appearance that combines a large nucleolus and a thickened nuclear membrane. The dermal component is arranged in short fascicules of melanocytes of similar cytology, difficult to visualize due to a massive infiltration of melanophages encased in a fibrous background.[1,2]

Two different PEM genotype models are presented in the 4th WHO classification of skin tumors (2018), one related to *PRKAR1A* inactivation and another associated with *PRKCA* fusion.[3]

Truncating mutations in *PRKAR1A* leading to the absence of protein production were first described in 2000 in the setting of the Carney complex.[4] Such tumors, often multiple in a germline carrier, have previously been described as 'epithelioid blue nevus'. So far, *BRAF* p.V600E mutations have been identified in their background, especially in combined cases.[5] *PRKAR1A* inactivation is considered a secondary event restricted to the PEM clone. In this study, we have explored the clinical, histological, and genetic background in a series of 22 cases of *PRKAR1A*-inactivated cutaneous melanocytic tumors.

Patients and Methods

Cases

The 21 cases of the cohort were retrieved from consultation cases from the Department of Biopathology at the Center Léon Bérard in Lyon, France (AF) in which PRKAR1A immunohistochemistry was performed for diagnostic purposes. Archival slides stained with hematoxylin and eosin or phloxin and the corresponding immunohistochemistry sections were re-examined for notable morphological characteristics. Morphological analysis and scoring of all cases were performed by AF, NM, and CC. Tumor size, growth kinetics, and anatomic location were obtained from the requisition form, and BRAF IHC, array-CGH, RNA sequencing, and (FISH) results included in the initial report were recorded.

For 8 cases, clinical follow-up information could be obtained from the referring pathologist or the clinician. The study was carried out according to the Declaration of Helsinki and has been approved by the research ethics committee of the Center Léon Bérard (ref: L21-05).

Histopathological and Immunohistochemical analysis

Hematoxylin-eosin and immunohistochemical staining were performed on 4 µm thick sections obtained from formalin-fixed paraffin-embedded tissues (FFPE). The Ventana BenchMark ULTRA system (Ventana, Tucson, USA) was used with the red coloring of the enhanced alkaline phosphatase red detection kit (Ventana; #800–031). The following antibodies were utilized: PRKAR1A (polyclonal rabbit, 1:200 NeoBiotech, Nanterre, France), Melan A (clone A103, 1:50, DAKO, Glostrup, Denmark), BRAF (Clone VE1, 1:100 Spring Bioscience, Pleasanton, CA).

RNA sequencing

RNA sequencing was performed in 12 cases.

Total RNAs were extracted from FFPE tissue sections using the FormaPure RNA kit (Beckman Coulter, Brea, CA, USA). A RNase-free DNase set (Qiagen, Courtaboeuf, France) was used to remove DNA. RNA quantification was evaluated using NanoDrop measurement (Thermo Fisher Scientific, Waltham, MA, USA) measurement and RNA quality using the DV200 value (the proportion of RNA fragments larger than 200nt) assessed using a TapeStation with Hs RNA Screen Tape (Agilent, Santa Clara, CA, USA). Samples with sufficient amount of RNA (> 0.5 µg) and quality (DV200 > 30%) were considered qualified for sequencing. 100 ng of total RNA was used to prepare each individual library with TruSeq RNA Exome (Illumina, San Diego, USA). 12 libraries were pooled at a concentration of 4nM each together with 1% PhiX. Sequencing was performed (paired end, 2 × 75 cycles) using NextSeq 500/550 high output V2 kit on a NextSeq 500 machine (Illumina).

The mean number of reads per sample was around 80 million. Alignments were performed using STAR on the GRCh38 version of the human reference genome. The number of duplicate reads was assessed using PICARD tools. Samples with a number of unique reads below 10 million (5 million paired reads) were discarded from the analysis. Fusion transcripts were called by five different algorithms, including STAR-Fusion, FusionMap, FusionCatcher, TopHat-Fusion and EricScript. Variant calling was performed using the GATK HaplotypeCaller, and filtering was achieved with the ANNOVAR annotation tool.

Array comparative genomic hybridization (aCGH)

DNA extraction was performed by macrodissecting FFPE tumor blocks followed by the use of the QIAamp DNA micro kit (Qiagen #56304, Hilden, De). Fragmentation and labeling were carried out according to the manufacturer's protocol (Agilent Technologies), using 1.5 µg of genomic DNA. Tumor DNA was labeled in Cy5, and a reference DNA with male or female sex-mismatch (Promega #G1471 and #G1521, Madison, USA) was labeled in Cy3. The labeled samples were then purified using KREApure columns (Agilent Technologies #5190-0418). The labeling efficiency was calculated using a Nanodrop ND2000 spectrophotometer. Cohybridization was performed on the 4 × 180K Agilent SurePrint G3 Human whole-genome design (Agilent Technologies # G4449A). The slides were washed, dried and scanned on the Agilent SureScan microarray scanner. The scan images were processed using Agilent Feature Extraction software V11.5 and the analysis was carried out using Agilent Genomic Workbench software V7.0.

Results

From an initial cohort of 43 cases of *PRKAR1A*-inactivated melanocytic tumors retrieved from the archives, a total of 21 cases showed an identified molecular driver. The 22 cases that were not included in the study lacked material for further analysis. Case n°17 was previously published.[6] Genetic, clinical, and histological data are summarized in **Table 1**. Full detailed results are available as supplementary data (**Suppl_table 1**).

Genetical findings

A wide spectrum of genetic backgrounds was found in the 21 *PRKAR1A*-inactivated tumors: *BRAF* p.V600E mutation in 9 cases (43%), *CYSLTR2* p.L129Q mutation in 4

cases (19%), rearrangement of *MAP3K8* in 2 cases (9%). Other anomalies were found only once: *GNAQ* p.Q209L, *MAP2K1* p.I103_K104del, *HRAS* p.G13R mutation and gene fusions including *KIF5B*::*RET*, *EPB41L1*::*MAP3K3* and *SLC16A6*::*PRKCA*.

BRAF mutations were identified by immunohistochemistry, and all other anomalies were identified by whole exome RNA sequencing. An array-CGH was performed in the case with *EPB41L1::MAP3K3* fusion and revealed ish cgh dim(17)(q23.2q25.1); reflecting a heterozygeous deletion of *PRKAR1A*. PRKAR1A mutations were detected in 5/12 cases by RNAseq and are detailed in **Suppl_table 1**.

Genetic subgrouping was attempted according to the WHO classification of cutaneous tumors and recent publications.[3,7,8] The 9 *BRAF*-mutated cases (43%) formed the 'common' subgroup (WHO class I), the 5 *GNAQ* and *CYSLTR2* mutated cases (24%) formed the 'blue' subgroup (WHO class VIII), the 4 gene fusions involving *RET*, *MAP3K8* and *MAP3K3,* the *HRAS* and *MAP2K1* mutated cases (28%) were clustered in the 'Spitz' subgroup (WHO class IV), while the *PRKCA* fused case remained isolated (WHO class I) (5%).

Clinical findings

No patient had multiple lesions or was clinically suspected of being the carrier of a germline *PRKAR1A* mutation such as described in the Carney complex. Globally, the patient's age ranged from 1 to 57 years (mean: 19 years) with a slight female predominance and no specific topography. The size of the lesions ranged from 2 to 8 mm (mean: 4 mm). The cases of the 'Spitz' subgroup were more predominant in children (range: 1-52 years ; median:11.5), cases of the 'common group' in young adults (range: 9-50 years ; median: 19), and the cases of the 'blue' subgroup in adults (range 17-57 years

old ; median: 34). Female predominance was present in the 'Spitz' subgroup (sex-ratio: 1M/5F). No trend was observed for a specific location for each subgroup.

The follow-up data did not show fatal or progressive disease in 8 patients. Follow-up ranged from 6 to 72 months with a median of 18 months. One child developed two perilesional metastases between the initial biopsy and the re-excision. Another child had a positive sentinel lymph node but a negative complementary nodal dissection without further signs of relapse during a 6 year follow-up. A patient diagnosed as melanoma with 2 positive lymph nodes surgically removed at the time of diagnosis received adjuvant immunotherapy and showed no signs of progression with a follow-up of 12 months.

Histopathological findings

Although important cytological and architectural variations were present, restriction of the analysis to each genetic subgroup showed more distinctive trends.

In the *PRKR1A*-inactivated 'common' subgroup (*BRAF* mutation), the 9 cases exhibited a combined/biphenotypic morphology. The prevalence of the PEM clone ranged from 40 to 90% compared to the remaining common nevus. The transition between common and hyperpigmented cells was abrupt, without intermediate cells (Figure 1A). Except for the malignant *PRKAR1A*-inactivated melanoma ex-nevus, the remaining 8 cases were slightly elevated, with limited or absent junctional component. The *PRKAR1A*-inactivated clone was most often superficial (7/8), or below the compound nevus in one case (Figure 1E, 1F). In most cases (6/8), the dermal component was organized in thin fascicules or isolated dermal cells, with epithelioid and spindled cytology. (Figure 1B) Pigmentation was important, with a predominance of melanophages over melanocytes

(6/8). No mitotic activity or high-grade atypia was present, except in the malignant case (Figure 1G, 1H).

In the *PRKR1A*-inactivated 'blue' subgroup, different morphological characteristics were observed: the silhouette was exophytic (4/5). Although the junctional component was often limited to a few nests, an important epidermal hyperplasia (3/5) was frequently associated (Figures 2A, 2G). The dermal architecture was organized in broad fascicules of most often spindled melanocytes, but with a predominance of melanocytes over melanophages (4/5). (Figures 2B, 2E, 2F, 2G, 2H) In a minority of cases (2/5), deep vertical cellular expansions were present, similar to those of cellular blue nevi (Figure 2C). Low mitotic activity was present in half of the cases.

In the *PRKR1A*-inactivated 'Spitz' subgroup, most cases (5/6) showed some degree of epidermal hyperplasia, with an endophytic and exophytic growth, resulting in a warty silhouette (Figure 3E, 3G). In 3/6 cases, large junctional nests were associated with these epidermal modifications. One case was combined (biphenotypic) with an adjacent compound Spitz nevus made of large spindle melanocytes that lacked pigmentation. The dermal component was constantly wedge-shaped, with broad fascicules of spindled and epithelioid melanocytes, which usually outnumbered melanophages (Figure 3A, 3B, 3C). Two cases contained multinucleated cells. Mitotic activity was usually low. Frequent images (4/6 cases) of vascular invasion were present (Insert in Figure 3B and 3F).

The unique case of *PRKCA*-fused melanocytic tumor showed an endophytic and exophytic silhouette, with epidermal hyperplasia associated with junctional nests. (Figure 4A). The nodular-shaped dermal component extended deeply, with a predominance of melanophages. Thin fascicules or isolated spindle and epithelioid melanocytes were difficult to visualize. Mitotic activity was absent.

Immunohistochemistry

The loss of PRKAR1A cytoplasmic expression was limited to the PEM clone in the 10 combined/biphenotypic cases, (Fig 1D) while it was lost in all melanocytes in the 11 other cases. (Figures 2D; 3G; 4D)

Expression of the B-Raf V600E-mutated protein was present in 9 cases, with diffuse cytoplasmic staining both in the common nevus and the hyperpigmented PEM clone.

MelanA (MART-1) staining was helpful to highlight the architecture of lesions obscured by an extensive melanophage infiltrate (Figure 4B).

Discussion

In this study, we have focused on PRKAR1A-inactivated PEM cases in which the genetic background could be assessed. This was only possible in 21 out of 43 cases, underscoring the difficulty to obtain such data, most often related to the small size and low cellularity of these tumors. Nine distinct genetic anomalies related to the respective genetic subgroups of common, Spitz, and blue nevi, as well as *PRKCA*-fused PEM were found associated. Although potentially confusing at first glance, these results are consistent with the existing literature on the subject.

In fact, the initial publications that described PEM were based on a purely morphological definition, namely hyperpigmentation and/or epithelioid dermal cytological features, but without genetic evidence of *PRKAR1A* inactivation, which is the molecular hallmark of PEM. Furthermore, most series tended to group cases with *PRKAR1A* inactivation, *PRKAR1A* mutation, and with *PRKCA* gene fusions all into the PEM group due to overlapping morphological features, although considered as two distinct types of melanocytic neoplasms according to the WHO classification.

PEM can occur in pure or combined form (biphenotypic) when accompanied by a nevus, consistent with the concept of melanocytoma introduced by the WHO classification. The definition of combined (biphenotypic) PEM is the co-occurrence of *PRKAR1A* inactivation on a nevus usually harboring a *BRAF* p.V600E mutation. Three cases similar to this definition have previously been described.[5] Our results support these data, showing a consistent association with a canonical *BRAF* mutation in our nine combined (biphenotypic) PEM cases.

Recently, 4 cases of melanoma have been reported with *BRAF* p.V600E mutations in a *PRKAR1A*-inactivated melanoma cohort.[9] These cases were considered as the malignant

transformation of combined PEMs, thus fitting the step-by-step tumor progression model from nevus to melanoma, with intermediate melanocytic lesions. One of our cases matches this description.

In 6 cases, a Spitz genetic background was identified and involved two *MAP3K8* fusions (*MAP3K8*::*DIP2C* and *MAP3K8*::*CCDC191*), a *EPB41L1*::*MAP3K3* fusion, a *KIF5B*::*RET* fusion, and *HRAS* p.G13R or *MAP2K1* p.I103_K104del mutations. In addition to the latter, these anomalies have not been reported so far in *PRKAR1A*-inactivated melanocytic proliferations. The spectrum of genetic anomalies associated with Spitz tumors has grown rapidly in recent years, many of which involve gene fusions of tyrosine kinase receptors (*ALK*, *ROS1*, *NTRK1*/2/3) and serine threonine kinase (*BRAF*, *MAP3K8*, *MAP3K3*).[13] Furthermore, *HRAS* and *MAP2K1* mutations are also described.[14,15] Here, we report the first occurrence of a combined (biphenotypic) lesion with a *MAP2K1* mutation. This is in part in agreement with previous publications of two variants of *PRKAR1A*-inactivated pure PEMs with such anomalies.[5] *MAP2K1* mutations have also been reported in nevi with a SPARK-like morphology[16] and in the genetic background of pure deep penetrating nevus (DPN).[17] It should be noted that combined DPN and combined *PRKAR1A*-inactivated PEM can both occur from the *BRAF*-mutated genetic background of common nevus.

Gene fusions in PEM have been reported twice with *NTRK3*: one case with a *MYO5A::NTRK3* fusion and a *PRKAR1A* mutation and another with a *SCAPER::NTRK3* fusion.[10,18] In both publications, data on PRKAR1A immunohistochemistry were unavailable. Also, the series of melanoma with *PRKAR1A*-inactivation found a *FAM39B*::*BRAF* fusion in one case, again underscoring the potential of such cases to

evolve towards malignancy.

In five of our cases, *PRKAR1A* inactivation was identified in association with a canonical mutation defining the blue nevi subgroup, namely *CYSLTR2* p.L129Q (4 cases) and *GNAQ* p.Q209L (1 case).

Although the association of *PRKAR1A* inactivation with *CYSLTR2* was previously unreported, lesions with PEM morphology and *GNAQ* mutations have been reported, but without testing PRKAR1A inactivation by immunohistochemical expression or genetic analyses.[10] Interestingly, the recent publication *PRKAR1A*-inactivated melanoma also reported 2 cases with *GNAQ* p.Q209L mutations.[9] This contributed to the debate on the possible combination of both alterations[12] in which the terminology of *PRKAR1A*-inactivated blue melanocytoma was suggested, while further genetic studies were pending.[11] Our data support this view as an independent subgroup and vouches for a specific new terminology for this novel combination of anomalies. Although we did not identify malignant cases, our group showed a range of atypia with clearly benign and intermediate-grade lesions.

Finally, we have identified a *PRKAR1A* inactivation in a *PRKCA*-fused PEM. In the WHO classification of skin tumors, the genetics associated with PEM include *PRKAR1A* mutations and *PRKCA* fusions, but not the combination of both. Although it has been pointed out that the *PRKCA* and *PRKAR1A* loci are closely mapped in the long arm of chromosome 17, we have not found a *PRKAR1A* inactivation in over 50 cases of *PRKC*-fused melanocytic lesions (data not shown), thus suggesting a true combination of both anomalies in our case. Morphologically, the lesion was rather typical of a *PRKCA*-fused tumor, with a hyperplastic epidermis and difficult to visualize epithelioid cytology, both present in the junction and dermis, with a massive melanophage infiltrate. We only

considered searching for the loss of PRKAR1A in this case because the RNA-seq data showed a low level of *PRKAR1A* expression.

PRKAR1A mutations were identified in 5/12 cases by RNA-seq (3 stop-gain, 1 frameshift, and 1 nonsynonymous mutation). This difficulty in identifying such mutations has been encountered in previous studies on the topic.[10,19] One factor could be the low cellularity in neoplastic melanocytes compared to adjacent keratinocytes and melanophages that dilute the anomaly combined with the small size of the lesions. Also, the range of anomalies leading to gene inactivation in a tumor suppressor gene is important (no hotspot anomaly) and could also involve gene fusions.

Although RNA-seq may not be the best tool for identifying all types of inactivating alterations, especially truncating mutations that induce loss of expression, or copy number alteration such as homozygous deletion (not explored in this study), it allowed us to confirm that *PRKAR1A* was underexpressed in 12 cases explored (data not shown). The usefulness of PRKAR1A immunohistochemistry in PEM is similar to what has been observed in other biphenotypic tumors such as BAP1-inactivated melanocytic tumors in which immunohistochemistry is a more potent screening tool compared to sequencing to assess genetic inactivation of a tumor suppressor gene.[20]

Although our series is limited in size, we attempted to analyze if clinical and morphological differences were present between genetic groups. Clinically, there were no differences in tumor size or location. Interestingly, trends were present in age categories in the various genetic subgroups: patients in the Spitz genetic group were mainly children, those in the *BRAF*-mutated group were mainly young adults, and those in the blue group were mainly adults. This distribution is consistent with the age variations found in lesions

without *PRKAR1A* inactivation.[3] Regarding morphological data, trends were also visible between genetic subgroups. *BRAF*-mutated lesions were combined, with a mainly intradermal architecture of the PEM component, organized in short fascicules, with epithelioid cytology, and most often difficult to visualize cells due to a dense melanophage infiltrate.

In the blue nevus group, the silhouette was exophytic and warty, with a variable junctional nested component. The dermal component was made of dense fascicules of more spindled than epithelioid cells with limited associated melanophages. A deep vertical expansion, as seen in cellular blue nevus, was only found in two cases.

In the Spitz-related genetic group, confluent junctional nests, hyperplastic epidermis, wedge-shaped silhouette, and larger dermal cellular bundles were present. These were readily visible compared to the 'common' *BRAF*-mutated subgroup, especially due to the much lower density of melanophages . Lastly, the presence of intravascular invasion was restricted to the Spitz group and was present in 4/6 cases. Two of such cases, with a *MAP3K8* or *MAP3K3* fusion, evolved with perilesional epidermotropic metastases or had sentinel lymph node involvement but without further evolution with a long follow-up in one case. Benton *et al.* recently emphasized in a review of PEM: "as with Spitz tumors, sentinel lymph node involvement from PEMs is common but distant metastasis or death of disease is extremely rare". Our findings directly link these two concepts. However, in light of these new data, it remains to be further studied whether PEMs with regional nodal involvement or local skin metastases demonstrate a Spitz genetic background, and in particular, what the frequency of *MAP3K8* or *MAP3K3* fusions is within this subgroup.

Altogether, our data support that the PEM morphology associated with *PRKAR1A* inactivation can occur in a wider genetic background than initially described, including common nevus, blue nevus, Spitz nevus, and *PRKCA*-fused PEM. This variety of genetic background suggests that this secondary genetic event is not restricted to a single group of nevi as previously suspected. The implications cover prognosis, treatment, and follow-up and require an update of the terminology of these lesions.

PRKAR1A-inactivated Pigmented Epithelioid Common Melanocytoma or Melanoma, *PRKAR1A*-inactivated Pigmented Epithelioid Blue Melanocytoma or Melanoma, and *PRKAR1A*-inactivated Pigmented Epithelioid Spitz Melanocytoma or Melanoma, are suggestions that require further collaborative confirmation as more cases are identified.

As a sidenote, a similar "genetic transversality" could be possible with all other morphology-modifying secondary genetic events. There is already such diversity in *BAP1*-inactivated melanocytic proliferations described in the common and blue groups as well as in *RASGRF2*-fused melanocytic tumors.[21,22(p2),23] This combination of patterns could also involve *CTNNB1* or *IDH1* mutations.[24]

Conclusion

In conclusion, our work supports the concept that *PRKAR1A* inactivation can potentially occur as a secondary event in melanocytic neoplasms harboring the genetic drivers of the common, Spitz and blue nevi subgroups. Lesions occur in the usual clinical setting of their group but show slightly different morphological characteristics. Given the few reported cases, this secondary event is presumed rare and occurs in small lesions with low cellularity possibly explaining the difficulties encountered so far to conceptualize a coherent molecular model.

References

1. Mandal RV, Murali R, Lundquist KF, et al. Pigmented epithelioid melanocytoma: favorable outcome after 5-year follow-up. *Am. J. Surg. Pathol.* 2009;33:1778–1782. doi:10.1097/PAS.0b013e3181b94f3c.

2. Zembowicz A, Carney JA, Mihm MC. Pigmented epithelioid melanocytoma: a low-grade melanocytic tumor with metastatic potential indistinguishable from animal-type melanoma and epithelioid blue nevus. *Am. J. Surg. Pathol.* 2004;28:31–40.

3. DE E, D M, RA S, et al. *WHO Classification of Skin Tumours*. Available at: http://publications.iarc.fr/Book-And-Report-Series/Who-Iarc-Classification-Of-Tumours/WHO-Classification-Of-Skin-Tumours-2018. Accessed November 4, 2018.

4. Kirschner LS, Sandrini F, Monbo J, et al. Genetic heterogeneity and spectrum of mutations of the PRKAR1A gene in patients with the carney complex. *Hum Mol Genet* 2000;9:3037–3046. doi:10.1093/hmg/9.20.3037.

5. Cohen JN, Joseph NM, North JP, et al. Genomic Analysis of Pigmented Epithelioid Melanocytomas Reveals Recurrent Alterations in PRKAR1A, and PRKCA Genes. *Am. J. Surg. Pathol.* 2017;41:1333–1346. doi:10.1097/PAS.0000000000000902.

6. Goto K, Pissaloux D, Paindavoine S, et al. CYSLTR2-mutant Cutaneous Melanocytic Neoplasms Frequently Simulate "Pigmented Epithelioid Melanocytoma," Expanding the Morphologic Spectrum of Blue Tumors: A Clinicopathologic Study of 7 Cases. *Am. J. Surg. Pathol.* 2019. doi:10.1097/PAS.0000000000001299.

7. Bahrami A, Lee S, Wu G, et al. Pigment-Synthesizing Melanocytic Neoplasm With Protein Kinase C Alpha (PRKCA) Fusion. *JAMA Dermatol* 2016;152:318–322. doi:10.1001/jamadermatol.2015.2524.

8. Quan VL, Zhang B, Mohan LS, et al. Activating Structural Alterations in MAPK Genes Are Distinct Genetic Drivers in a Unique Subgroup Of Spitzoid Neoplasms. *Am J Surg Pathol* 2019;43:538–548. doi:10.1097/PAS.0000000000001213.

9. Cohen JN, Yeh I, Mully TW, et al. Genomic and Clinicopathologic Characteristics of PRKAR1A-inactivated Melanomas: Toward Genetic Distinctions of Animal-type Melanoma/Pigment Synthesizing Melanoma. *Am J Surg Pathol* 2020;44:805–816. doi:10.1097/PAS.0000000000001458.

10. Isales MC, Mohan LS, Quan VL, et al. Distinct Genomic Patterns in Pigmented Epithelioid Melanocytoma: A Molecular and Histologic

Analysis of 16 Cases. *Am J Surg Pathol* 2019;43:480–488. doi:10.1097/PAS.0000000000001195.

11. Cohen JN, Yeh I, Mully TW, et al. Response To: Feasibility of a Tumor Progression Model in PRKAR1A-inactivated Melanomas. *The American Journal of Surgical Pathology* 2021;45:869–870. doi:10.1097/PAS.0000000000001721.

12. Saggini A. Feasibility of a Tumor Progression Model in PRKAR1A-inactivated Melanomas. *The American Journal of Surgical Pathology* 2021;45:868–869. doi:10.1097/PAS.0000000000001648.

13. The role of gene fusions in melanocytic neoplasms - Quan - 2019 - Journal of Cutaneous Pathology - Wiley Online Library. Available at: https://onlinelibrary.wiley.com/doi/10.1111/cup.13521. Accessed October 14, 2021.

14. Bastian BC, LeBoit PE, Pinkel D. Mutations and copy number increase of HRAS in Spitz nevi with distinctive histopathological features. *Am. J. Pathol.* 2000;157:967–972. doi:10.1016/S0002-9440(10)64609-3.

15. Sunshine JC, Kim D, Zhang B, et al. Melanocytic Neoplasms With MAP2K1 in Frame Deletions and Spitz Morphology. *Am J Dermatopathol* 2020;42:923–931. doi:10.1097/DAD.0000000000001795.

16. Donati M, Nosek D, Waldenbäck P, et al. MAP2K1-Mutated Melanocytic Neoplasms With a SPARK-Like Morphology. *Am J Dermatopathol* 2021;43:412–417. doi:10.1097/DAD.0000000000001840.

17. Yeh I, Lang UE, Durieux E, et al. Combined activation of MAP kinase pathway and ß-catenin signaling cause deep penetrating nevi. *Nat Commun* 2017;8:644. doi:10.1038/s41467-017-00758-3.

18. A pediatric case of pigmented epithelioid melanocytoma with chromosomal copy number alterations in 15q and 17q and a novel NTRK3-SCAPER gene fusion - Friedman - 2020 - Journal of Cutaneous Pathology - Wiley Online Library. Available at: https://onlinelibrary.wiley.com/doi/10.1111/cup.13566. Accessed October 13, 2021.

19. Zembowicz A, Knoepp SM, Bei T, et al. Loss of expression of protein kinase a regulatory subunit 1alpha in pigmented epithelioid melanocytoma but not in melanoma or other melanocytic lesions. *Am J Surg Pathol* 2007;31:1764–1775. doi:10.1097/PAS.0b013e318057faa7.

20. Cabaret O, Perron E, Bressac-de Paillerets B, et al. Occurrence of BAP1 germline mutations in cutaneous melanocytic tumors with loss of BAP1-

expression: A pilot study. *Genes Chromosomes Cancer* 2017;56:691–694. doi:10.1002/gcc.22473.

21. Wiesner T, Obenauf AC, Murali R, et al. Germline mutations in BAP1 predispose to melanocytic tumors. *Nat Genet* 2011;43:1018–1021. doi:10.1038/ng.910.

22. Houlier A, Pissaloux D, Tirode F, et al. RASGRF2 gene fusions identified in a variety of melanocytic lesions with distinct morphological features. *Pigment Cell Melanoma Res* 2021. doi:10.1111/pcmr.13004.

23. Costa S, Byrne M, Pissaloux D, et al. Melanomas Associated With Blue Nevi or Mimicking Cellular Blue Nevi: Clinical, Pathologic, and Molecular Study of 11 Cases Displaying a High Frequency of GNA11 Mutations, BAP1 Expression Loss, and a Predilection for the Scalp. *Am J Surg Pathol* 2016;40:368–377. doi:10.1097/PAS.0000000000000568.

24. Macagno N, Pissaloux D, Etchevers H, et al. Cutaneous Melanocytic Tumors With Concomitant NRASQ61R and IDH1R132C Mutations: A Report of 6 Cases. *Am. J. Surg. Pathol.* 2020;44(10):1398-1405. doi:10.1097/PAS.0000000000001500.

Figures

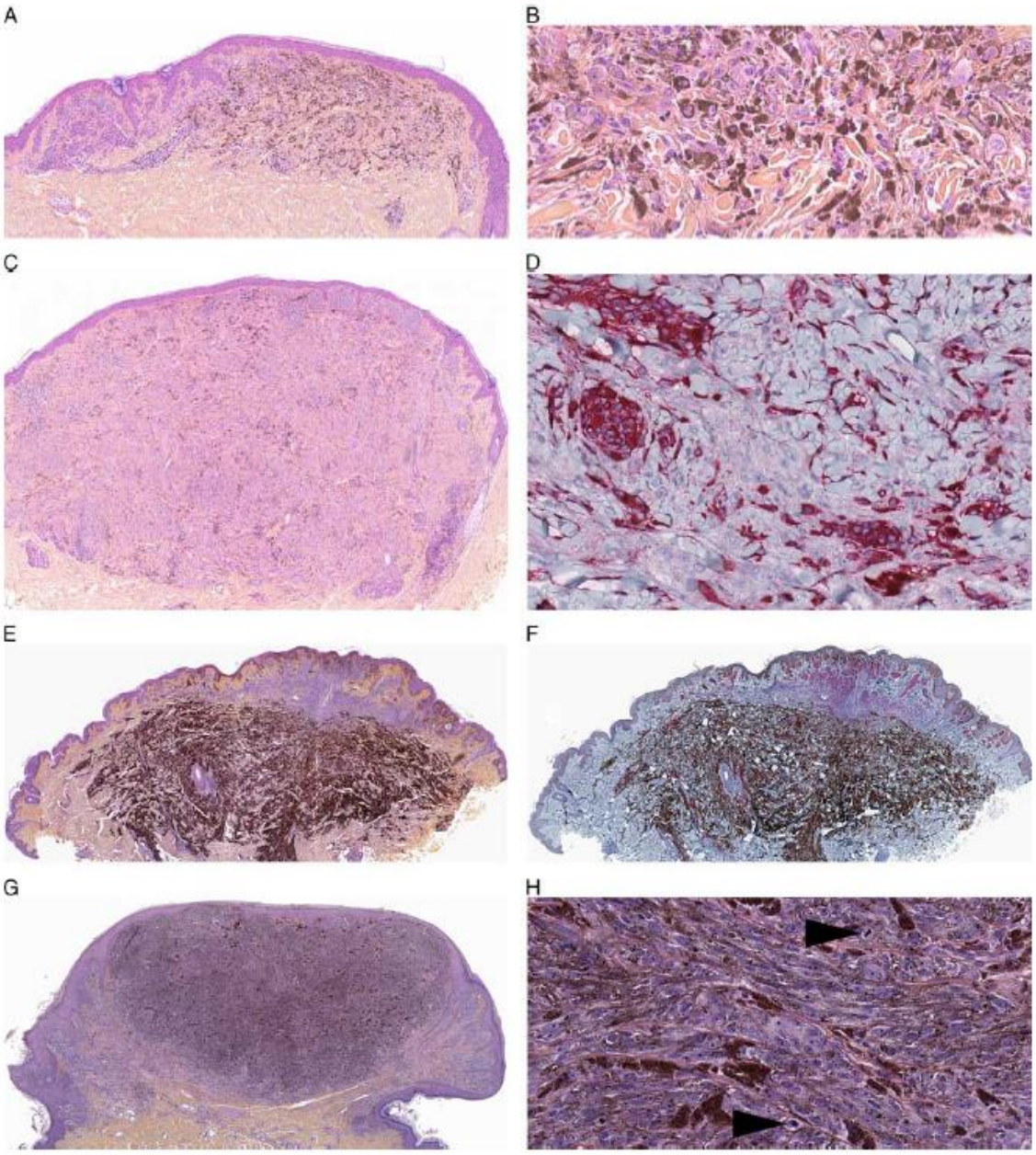

Figure 1 PRKAR1A-inactivated combined melanocytic proliferation with a *BRAF* p.V600E mutation

A: Combined/bi-phenotypic architecture with on the left side a common compound nevus and on the right side a hyperpigmented mainly dermal clone forming a horizontal band. (Case 1)**. B**: close-up view of A: isolated or small clusters of epithelioid cells with fried

egg nuclei surrounded by numerous melanophages. **C**: Combined/bi-phenotypic architecture with a few nests of common nevus near the junction and a mainly dermal nodular clone with overall low pigmentation (Case 6). **D**: PRKAR1A immunohistochemistry with strong cytoplasmic staining of the common nevus nests and lack of expression in the epithelioid melanocytes visible on blue counterstain (Case 6). **E**: Combined/bi-phenotypic architecture with a wedge-shaped pigmented clone underneath the common compound nevus (Case 8). **F**: BRAF V600E immunohistochemistry positive in both components underscoring the low density in the pigmented clone mainly formed of melanophages. **G:** Malignant melanoma ex-nevus. Exophytic silhouette with a dense upper dermis nodule (Case 2). **H**: close-up view of G: dense fascicules of atypical epithelioid and spindled melanocytes with high mitotic activity (arrows).

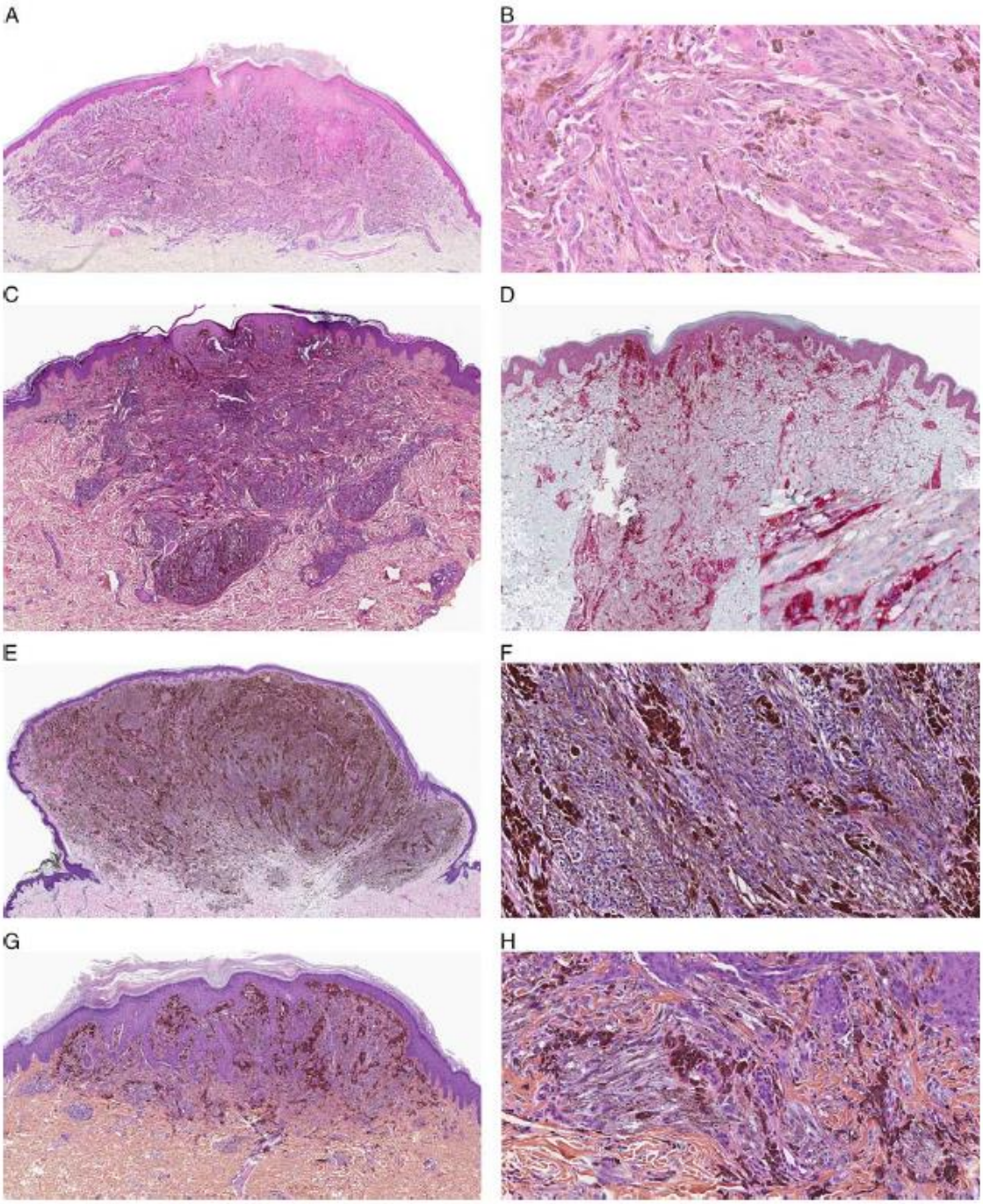

Figure 2 PRKAR1A-inactivated melanocytic proliferation with blue nevus genetic background

A: Epidermal hyperplasia with dermal wedge-shaped silhouette (Case 16; *GNAQ* p.Q209L mutation). **B**: Close up view of A, large fascicules of epithelioid melanocytes

outnumbering melanophages. **C**: Mild epidermal hyperplasia; dumbell vertical dermal expansion of large fascicules, moderate pigmentation (Case 19; *CYSLTR2* p.L129Q mutation). **D**: PRKAR1A immunohistochemistry. Complete loss of cytoplasmic expression. Insert with close-up view showing epithelioid and spindled cytology on counter stain. **E**: Exophytic silhouette with large dermal fascicular architecture (Case 20; *CYSLTR2* p.L129Q mutation) **F**: Close-up view of E underscoring the spindled cytology of the fascicules. **G**: Compound, slightly elevated, fasciculated melanocytic proliferation with a few junctional nests and epidermal hyperplasia (Case 21; CYSLTR2 p.L129Q mutation). **H**: close-up view of G: dermal component made of fascicules of medium-sized spindled melanocytes.

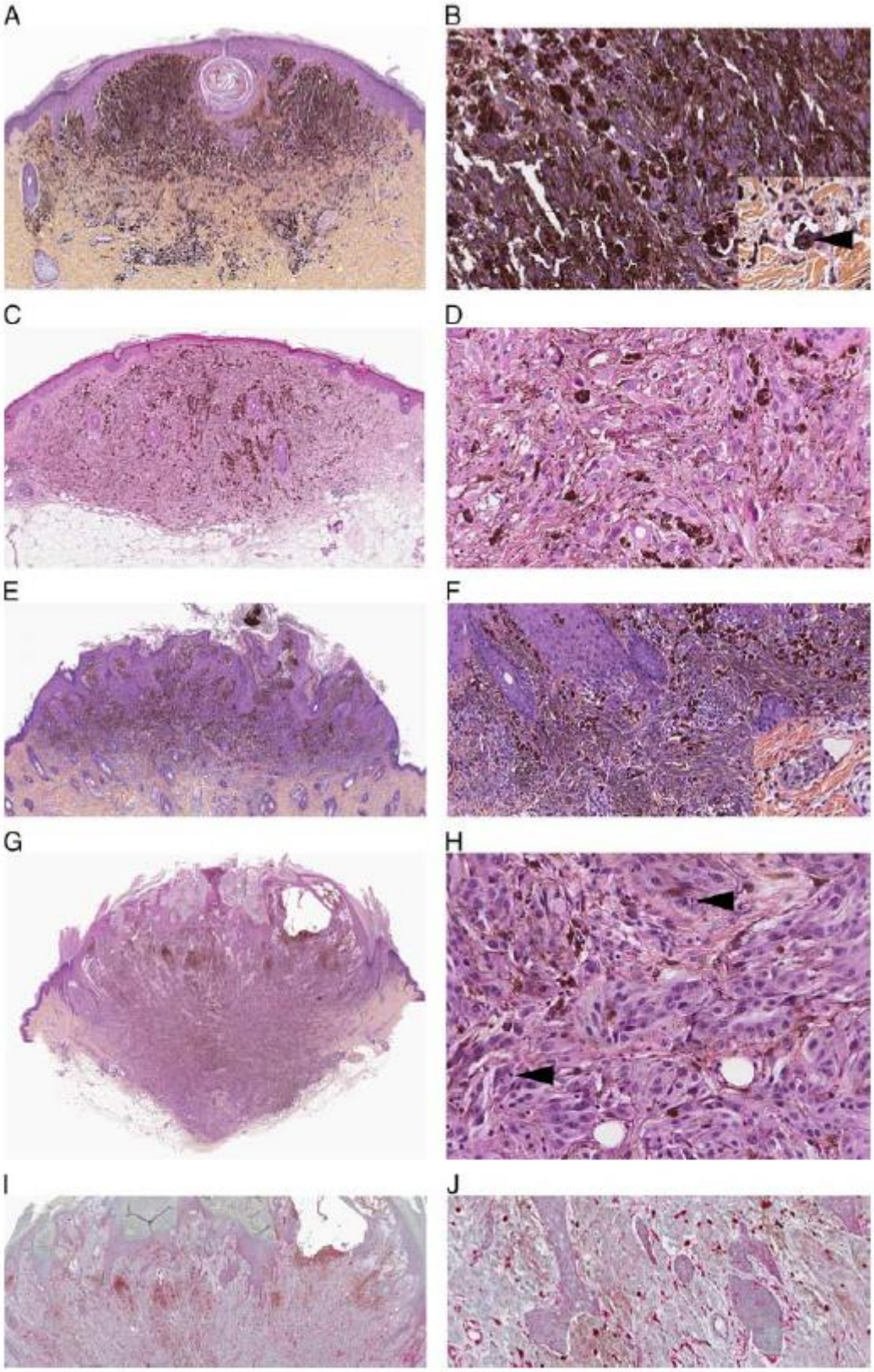

Figure 3. PRKAR1A-inactivated melanocytic proliferation with Spitz nevus genetic

background

A: Slightly elevated hyperplastic epidermis encasing dense sheets of hyperpigmented cells. Wedge-shape architecture. (Case 12 with a *MAP3K8::CCDC191* translocation) **B**: Close-up view of A: dense sheet area made of spindled hyperpigmented melanocytes. Insert showing peripheral intravascular invasion (arrow). **C:** Mainly dermal, dense, wedge-shaped, mildly pigmented melanocytic proliferation extending to the subcutis. (Case 14 with *HRAS* p.G13R mutation). **D**: Close-up view of C: Dense sheets of epithelioid melanocytes with few melanophages. **E**: Warty epidermal hyperplasia encasing junctional nests of pigmented melanocytes (Case 13 with *KIF5B::RET* translocation). **F**: Close-up view of E: Fascicules of medium-sized spindled melanocytes in the junction and upper dermis. Insert showing peripheral intravascular invasion. **G**: Large warty epidermal hyperplasia with wedge-shaped dermal silhouette. (Case 15 with *EPB41L1::MAP3K3* translocation). **H**: Close-up view of G: dense fascicules of epithelioid melanocytes with mitotic figures (arrows). Few melanophages. **I-J**: PRKAR1A immunohistochemistry with global and close-up views showing complete loss of cytoplasmic expression in the melanocytes.

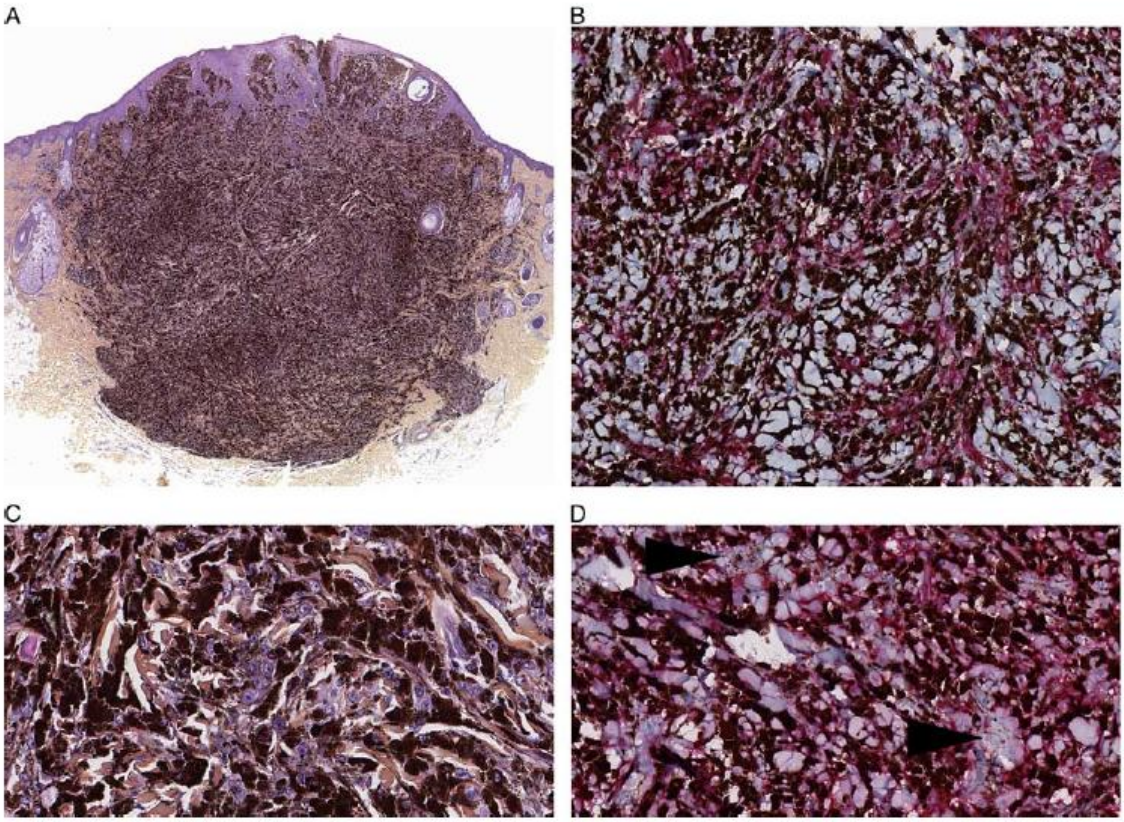

Figure 4. PRKAR1A-inactivated melanocytic proliferation with PRKCA-fusion (case 22)

A: compound, mainly dermal, hyperpigmented proliferation with a slightly elevated hyperplastic epidermis. **B**: MelanA immunohistochemistry highlighting the small clusters or isolated melanocytes stretched-out between dense patches of melanophages. **C**: high power view showing typical fried-egg nuclei. **D**: PRKAR1A immunohistochemistry with unstained clusters of epithelioid cells (Arrow).